Geomechanics and Engineering, *Vol. 24, No. 6 (2021) 545-557*
DOI: https://doi.org/10.12989/gae.2021.24.6.545

Vibration of multilayered functionally graded deep beams under thermal load

Abdullateef H. Bashiri[1], Şeref D. Akbaş[2], Alaa A. Abdelrahman[3], Amr Assie[1,3], Mohamed A. Eltaher[*4,5] and Elshahat F. Mohamed[6]

[1]*Department of Mechanical Engineering, Faculty of Engineering, Jazan University, P. O. Box 45142, Jazan, Kingdom of Saudi Arabia*
[2]*Department of Civil Engineering, Bursa Technical University, 16330, Bursa, Turkey*
[3]*Department of Mechanical Design & Production, Faculty of Engineering, Zagazig University,P.O. Box 44519, Zagazig, Egypt*
[4]*Department of Mechanical Engineering, Faculty of Engineering, King Abdulaziz University, P.O. Box 80204, Jeddah, Saudi Arabia*
[5]*Department of Mechanical Design & Production, Faculty of Engineering, Zagazig University,P.O. Box 44519, Zagazig, Egypt*
[6]*Department of Mechanical Power, Faculty of Engineering, Zagazig University,P.O. Box 44519, Zagazig, Egypt*

(Received September 12, 2020, Revised March 13, 2021, Accepted March 17, 2021)

Abstract. Since the functionally graded materials (FGMs) are used extensively as thermal barriers in many of applications. Therefore, the current article focuses on studying and presenting dynamic responses of multilayer functionally graded (FG) deep beams placed in a thermal environment that is not addressed elsewhere. The material properties of each layer are proposed to be temperature-dependent and vary continuously through the height direction based on the Power-Law function. The deep layered beam is exposed to harmonic sinusoidal load and temperature rising. In the modelling of the multilayered FG deep beam, the two-dimensional (2D) plane stress continuum model is used. Equations of motion of deep composite beam with the associated boundary conditions are presented. In the frame of finite element method (FEM), the 2D twelve-node plane element is exploited to discretize the space domain through the length-thickness plane of the beam. In the solution of the dynamic problem, Newmark average acceleration method is used to solve the time domain incrementally. The developed procedure is verified and compared, and an excellent agreement is observed. In numerical examples, effects of graduation parameter, geometrical dimension and stacking sequence of layers on the time response of deep multilayer FG beams are investigated with temperature effects.

Keywords: transient response; forced vibration; thermal effect; deep beam; multilayered functionally graded; finite element method

1. Introduction

During 1984 in Japan, through the space-plane project, a new class of composite material known as functionally graded material (FGM) was invented and exploited as a thermal barrier, Alshorbagy (2011). FGMs are nonhomogeneous materials whose properties are altered in a particular direction according to some laws so that their properties can better meet the designers' needs, Hamed *et al.* (2020a). FGMs have earned significant importance in extremely high-temperature environments such as nuclear reactors, gas turbine, chemical plants, experimental thermonuclear reactor and the semiconductor industry, Ueda and Mizusawa (2020). FGMs have been used in many other applications such as aerospace, optics, biomedical, automotive, micro/nano-electro-mechanical system (MEMS/NEMS) and atomic force microscopes (AFMs), Eltaher *et al.* (2013a&b).

Yang *et al.* (2008) studied analytically free and forced vibrations of inhomogeneous open edge cracks beams subjected to an axial compressive force. Şimşek and Kocatürk (2009) and Şimşek (2010) investigated free vibration characteristics and dynamic behaviors of FG simply supported beams under a concentrated moving harmonic load. Assie *et al.* (2011) developed an efficient numerical algorithm to investigate the dynamic transient response of orthotropic viscoelastic composite laminates under step-pulse and sin-pulse forces. Sedighi *et al.* (2012) presented six different analytical approaches to investigate and solve the governing equation of nonlinear vibration of cantilever beams. Hemmatnezhad *et al.* (2013) exploited finite element formulation to study large-amplitude free vibrations of FG beams. Sedighi (2014) and Sedighi *et al.* (2015) studied dynamic pull-in instability of vibrating electrically actuated microbeams based on the strain gradient elasticity theory. Gan *et al.* (2015) presented a finite element procedure for dynamic analysis of non-uniform Timoshenko beams made of axially FGM under multiple moving point loads. Sedighi and Bozorgmehri (2016) explored the dynamic instability of doubly clamped cylindrical nanowires in the presence of Casimir attraction and surface effects by using the modified couple stress theory. Hosseini and Rahmani (2016) studied free vibration of shallow and deep curved FG nanobeam via a nonlocal Timoshenko curved beam model. Akbaş (2016, 2017a) exploited modified couple stress theory to investigate the dynamic response of simply supported viscoelastic nanobeams resting on Winkler-Pasternak elastic foundation and excited by a transverse triangular impulse force. Akbaş

∗Corresponding author, Professor
E-mail: meltaher@kau.edu.sa, mmeltaher@zu.edu.eg

ISSN: 2005-307X (Print), 2092-6219 (Online)

(2017) investigated the effects of temperature rising on porous FGM deep beams' free vibration. Akbaş (2018a&b) modified his previous model to include the crack effect on the dynamic response of nanobeams' viscoelastic behaviours. Akbaş (2018c) investigated free and forced vibration of a bi-material composite beam. Albino *et al.* (2018) studied nonlinear dynamic behaviors of risers manufactured with FGMs and modelled by 3D beam element. Dinh Duc *et al.* (2018) predicted nonlinear dynamic response of FG porous plates resting on elastic foundation and subjected to thermal and mechanical loads.

Akbaş (2019a) studied the nonlinear FG cantilever beam's under non-uniform hygrothermal effect and exploited the finite element method and Newton-Raphson method with incremental displacement to solve the proposed model. Akbaş (2019b) analyzed forced vibration of deep sandwich beams made of sandwich FGM including porosity effects. Abdalrahmaan *et al.* (2019) and Almitani *et al.* (2019) developed a unified mathematical model to investigate free and forced vibration responses of perforated thin and thick beams. Hamed *et al.* (2019) studied FG porous nanobeams bending behaviours with four types of porosity using nonlocal elasticity theory. Rajasekaran and Khaniki (2019) studied size-dependent forced vibration of non-uniform bi-directional FG beams embedded in an elastic environment and carrying a moving harmonic mass. Ebrahimi *et al.* (2019) investigated the frequency response of curved embedded magneto-electro-viscoelastic functionally graded nano-beams. Mohamed *et al.* (2019) and Emam *et al.* (2019) studied analytically post-buckling of imperfect nanobeam using classical Euler beam theory. Berghouti *et al.* (2019) studied the dynamic behavior of FG porous nano-beams based on nonlocal n^{th}-order shear deformation theory. Tsiptsis and Sapountzaki (2019) presented the generalized warping and distortional problem of straight or horizontally curved composite beams of arbitrary cross-section, loading and boundary conditions. Ahmadi and Foroutan (2019) presented the effect of the multi vibration absorbers on the nonlinear FG beam under periodic load with various boundary conditions. Rahman *et al.* (2019) investigated forced nonlinear vibration of Euler-Bernoulli beam resting on a nonlinear elastic foundation by using a modified multi-level residue harmonic balance method. Almitani *et al.* (2020), Eltaher and Abdelrahmaan (2020) and Abdelrahmaan *et al.* (2020a) presented the surface energy effects on bending and buckling of perforated nanobeam. Eltaher *et al.* (2020a) presented a static stability analysis of unified composite beams under varying axial loads. Eltaher and Mohamed (2020) and Hamed *et al.* (2020b) investigated the sandwich composite beam's buckling under varying axial loads with and without elastic foundations. Akbaş *et al.* (2020a, b) presented a comprehensive model to investigate FG porous thick beam's vibration response under the dynamic sine pulse load, including the damping effect and viscoelastic support. Hamidi *et al.* (2020) investigated forced axial vibration of micro and nanobeam under axial harmonic moving and constant distributed forces via nonlocal strain gradient theory. Abo-bakr *et al.* (2020, 2021a, b) exploited multi-objective shape optimization to get the optimum weight of FG microbeam under static and dynamic stability effects. In the nonlocal strain gradient framework, She (2020) investigated the wave propagation of FG reinforced polymeric composite nanoplates. She *et al.* (2021) studied the forced vibration response of curved reinforced microbeams using the modified strain gradient theory. Alnujaie *et al.* (2021) studied forced vibration of a functionally graded porous beam resting on a viscoelastic foundation. Assie *et al.* (2021) investigate the dynamic responses of thick Timoshenko perforated beams under a moving load using Ritz method.

Based on the usage of the thermal barrier and thermal protector as the main objective of FGM. Therefore, many researchers have considered the existence of the instability and dynamic behaviors of FG structures during service life where temperature variations exist. Lee and Erdogan (1994) explained residual and thermal stresses in FGM and laminated thermal barrier coatings. Xiang and Yang (2008) studied free and forced vibrations of sandwich FG beam of variable thickness under thermally induced initial stresses within the framework of Timoshenko beam theory. Doroushi *et al.* (2011) investigated free and forced vibration characteristics of a FG beam under thermo-electro-mechanical loads using the higher-order shear deformation beam theory. Malekzadeh and Monajjemzadeh (2013) investigated linear and nonlinear dynamic responses of FG plates in a thermal environment under moving load including the effects of initial thermal stresses and elastic foundations. Zenkour and Abouelregal (2014) investigated the effect of two temperatures on FG nanobeams subjected to sinusoidal pulse heating sources using Laplace transformation domain. Barka *et al.* (2016) examined sandwich plates' post-buckling behaviour with FG face sheets under uniform temperature rise loading based on sinusoidal shear deformation theory. Emam and Eltaher (2016) presented influences of temperature variation and moisture absorption on the buckling and post-buckling of composite beams in hydrothermal environments. Wang and Wu (2016) studied the dynamic response of an axially FG beam under a thermal environment and subjected to a moving harmonic load within frameworks of classical and Timoshenko beam theories.

Ghadiri *et al.* (2017) studied the vibration of a rotary FG plate considering thermal and Coriolis effects. Mirjavadi *et al.* (2017) illustrated the thermo-mechanical vibration behavior of two dimensional functionally graded porous nanobeam according to the power-law function. Attia *et al.* (2018) and Eltaher *et al.* (2018) analyzed the thermoelastic crack pipe manufactured by FGM and conveyed natural gas using the finite element method. Karami *et al.* (2018) exploited nonlocal higher-order shear deformation beam theory to study thermal buckling of porous FG nanobeam integrated with piezoelectric sensor and actuator. Soliman *et al.* (2018) studied nonlinear transient analysis of FG pipe subjected to internal pressure and unsteady temperature. Arioui *et al.* (2018) presented thermal buckling of FGM beams with parabolic thickness variation and temperature-dependent materials. Chen *et al.* (2018) investigated thermo-elastic vibration behaviors of FGM beams with general boundary conditions by using a higher-order shear

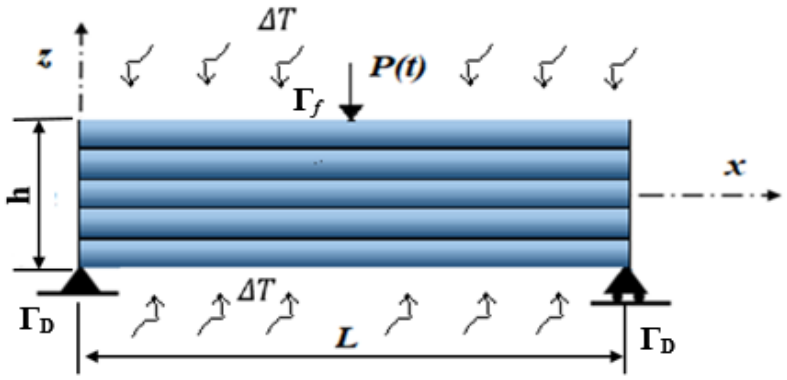

Fig. 1 A simply supported multilayered functionally graded deep beam under thermomechanical loading.

deformation beam theory. Salah *et al.* (2019) presented the influence of thermal load on buckling of ceramic-metal FGM sandwich plates using a 2D integral plate model. Ganczarski and Szubartowski (2019) demonstrated conditions of stress-free deformation of anisotropic FGM interface under thermal loading. Abdulrazzaq *et al.* (2020) studied thermal buckling of nonlocal clamped FG plate exponentially according to a secant function. Ebrahimi *et al.* (2020) developed an analytical formulation and solution process for buckling porous magneto-electro-elastic FG beam analysis via different thermal loadings and various boundary conditions. Esen *et al.* (2021) studied a vibration of FG cracked beam in microsize under the thermal and magnetic environments.

According to previous works and reviews, the dynamic response of multilayer FG deep beams with material-temperature dependent properties has not been studied elsewhere. Thus, the current article tries to fill this gap and investigates this topic in detail. 2D plane stress constitutive model models the deep FG beam. Finite element model and Newmark time integration are exploited to solve the mathematical model. The rest of the article is arranged as following: - constitutive equations, problem formulation, and numerical procedure are presented in Section 2. Section 3 is devoted to validation and parametric studies to illustrate influences of graduation parameter, geometrical dimension and stacking sequence of layers on the time response of deep multilayer FG beams are investigated with temperature effects. Section 4 presents the main remarks and highlighted points.

2. Problem formulation

2.1 Functionally graded material model

Consider a supported multilayered functionally graded deep beam with five functionally graded layers subjected to thermomechanical loading, as shown in Fig.1. The beam has a span length, *L,* thickness*, t,* and depth *h*. A Perfect bond is assumed between layers. Additionally, the functionally graded layers have the same thickness and are located symmetrically according to the mid-plane axis. Each layer has graduation material properties, *P*, (i.e., Elasticity modulus *E*, Poisson's ratio ν, thermal expansion coefficient α, thermal conductivity *k* and mass density ρ) graded along the thickness direction according to the Power-Law function, Attia *et al.* (2018); Attia and Abdelrahman (2018)

Table 1 The coefficients of temperature T for Zirconia (Reddy and Chin 1998)

The material properties	P_0	P_{-1}	P_1	P_2	P_3
Thermal expansion coefficient $\alpha(1/K)$	12.766×10^{-6}	0	-1.491×10^{-3}	1.0006×10^{-5}	-6.778×10^{-11}
Young's modulus E (Pa)	244.27×10^{9}	0	-1.371×10^{-3}	1.214×10^{-6}	-3.681×10^{-10}
Poisson's ratio ν	0.2887	0	1.133×10^{-4}	0	0
Mass density ρ (kg/m^3)	5700	0	0	0	0
Coefficient of thermal conductivity k (W/mK)	1.700	0	1.276×10^{-4}	6.648×10^{-8}	0

Table 2 The coefficients of temperature T for Aluminum Oxide (Reddy and Chin 1998)

The material properties	P_0	P_{-1}	P_1	P_2	P_3
Thermal expansion coefficient $\alpha(1/K)$	6.8269×10^{-6}	0	1.838×10^{-4}	0	0
Young's modulus E (Pa)	349.55×10^{9}	0	-3.853×10^{-4}	4.027×10^{-7}	-1.673×10^{-10}
Poisson's ratio ν	0.26	0	0	0	0
Mass density ρ (kg/m^3)	2700	0	0	0	0
Coefficient of thermal conductivity k (W/mK)	-14.087	-1123.6	$-6.227\text{x}10^{-3}$	0	0

$$P(z,T) = \Delta P(z,T)\left[\frac{z}{h}+\frac{1}{2}\right]^{n} + P_B(z,T), \quad \text{and } \Delta P(z,T) = P_T(z,T) - P_B(z,T) \tag{1a}$$

where n refers to the material graduation exponent, T is the absolute temperature. The subscripts B and T refer to the bottom and top sides of the functionally graded layer, respectively.

On the other hand, the temperature dependency of the material properties is described by the following nonlinear function, Touloukian (1966):

$$P(T) = P_0\ (P_{-1}\ T^{-1} + 1 + P_1 T + P_2\ T^2 + P_3\ T^3) \tag{1b}$$

in which the absolute temperature, $T = T_0 + \Delta T$, where T_0 is the reference room temperature and ΔT is the temperature change. The polynomial coefficients, P_{-1}, P_0, P_1, P_2 *and* P_3

indicate the temperature parameters. Throughout the analysis of all cases in this study, the FGM deep beam is considered to be made of Zirconia and Aluminum. The material temperature-dependent coefficients for Zirconia and Aluminum are presented in Table 1 and 2, Reddy and Chin (1998).

2.2 Thermal effect

Assuming that the deep beam is subjected to the temperature effect. The temperature rise $\Delta T = \Delta T(z)$ is governed by the heat transfer equation of, Akbaş (2017b)

$$-\frac{d}{dz}\left[k(z)\frac{d\Delta T(z)}{dz}\right]=0 \tag{2}$$

in which $k(z)$ is the thermal conductivity coefficient that is temperature-independent, by integrating Eq. (2) using boundary conditions $\Delta T(h/2) = \Delta T_T$ and $\Delta T(-h/2) = \Delta T_B$, the following expression can be obtained, Reddy and Chin (1998):

$$\Delta T(z)=\Delta T_B+\left(\Delta T_T-\Delta T_B\right)\int_{-h/2}^{z}\frac{1}{k(z)}dz\Big/\int_{-h/2}^{h/2}\frac{1}{k(z)}dz \tag{3}$$

2.3 Kinematic and constitutive relations

The beam span to thickness ratio is selected to be small. The 2D plane stress continuum model could be employed to describe the multilayered FG deep beam thermomechanical behaviour. Based on the 2D plane stress assumption, the kinematic strain-displacement relations are given by

Abdelrahman and Elshafei (2020)
$$\begin{Bmatrix}\varepsilon_{xx}\\ \varepsilon_{zz}\\ \gamma_{xz}\end{Bmatrix}=\begin{bmatrix}\frac{\partial}{\partial x} & 0\\ 0 & \frac{\partial}{\partial z}\\ \frac{\partial}{\partial z} & \frac{\partial}{\partial x}\end{bmatrix}\begin{Bmatrix}u\\ w\end{Bmatrix} \tag{4}$$

where u, w are respectively the displacements in x and z directions. ε_{xx} and ε_{zz} are the normal in-plane strains components, and γ_{xz} is the shear in-plane strain. The constitutive relations for the temperature -dependent FG layer can be written as Reddy and Chin (1998)

$$\begin{Bmatrix}\sigma_{xx}\\ \sigma_{zz}\\ \tau_{xz}\end{Bmatrix}=\begin{bmatrix}C_{11}(z,T) & C_{12}(z,T) & 0\\ C_{12}(z,T) & C_{22}(z,T) & 0\\ 0 & 0 & C_{33}(z,T)\end{bmatrix}\begin{Bmatrix}\varepsilon_{xx}-\alpha(z,T)\Delta T(z)\\ \varepsilon_{zz}-\alpha(z,T)\Delta T(z)\\ \gamma_{xz}\end{Bmatrix} \tag{5}$$

where the stiffness can be described as functions of elasticity and Poisson's ratio as following:

$$C_{11}(z,T)=C_{22}(z,T)=\frac{E(z,T)}{1-[\nu(z,T)]^2},\ C_{33}(z)=\frac{E(z,T)}{2\ [1+\nu(z,T)]};\quad C_{12}(z)=\frac{\nu(z,T)E(z,T)}{1-[\nu(z,T)]^2} \tag{6}$$

2.4 Governing differential equation of motion

Consider the domain of the deep multilayerd beam refered to as Ω bounded by the boundary Γ. The Cartesian coordinates $\boldsymbol{x^T}=[x,z]^T$ are used to describe infinitesimal deformation. The dynamic equilibrium requires, Wanga and Qin (2008)

$$\sigma_{ij,j}+b_i=\rho(z,T)\ddot{U}\ \text{ in }\ \Omega, \tag{7}$$

where $\sigma_{ij,j}$ denotes the components of Cauchy stress tensor and b_i is the components of body force per unit volume. The associated kinematic and kinematic boundary conditions are given by

$$u_i=\bar{u}_i\ \text{ on }\ \Gamma_D, and\quad t_i=\sigma_{ij}n_j=\bar{t}_i\ \text{ on }\ \Gamma_f \tag{8}$$

where $\bar{u}_i$ is the prescribed the displacements on Γ_D and $\bar{t}_i$ is the given tractions on Γ_f. Γ_D and Γ_f are complementary parts of the boundary Γ. n_j represents the direction cosines of the unit outward normal to the boundary.

3. Finite element formulation

Based on Hamilton's procedure, the dynamic equilibrium equation can be depicted as,

$$\int_\Omega \delta\varepsilon^T\sigma d\Omega-\int_\Omega[B]^T\{\sigma^{th}\}d\Omega-\int_\Omega\delta U^T\left[\boldsymbol{b}-\rho\ddot{U}\right]^T d\Omega-\int_\Gamma\delta U^T P(t)d\Gamma=0 \tag{9}$$

where Ω is the occupied domain of the body, Γ is the boundary domain, $\boldsymbol{b}$ is the body force, and δU is the generalized virtual displacement. This equation can be represented in terms of displacement field and stiffness coefficients as follows, Gupta and Talha (2015):

$$\begin{aligned}\int_A\Big[&C_{11}(z,T)\frac{\partial u}{\partial x}\frac{\partial\delta u}{\partial x}+C_{22}(z,T)\frac{\partial w}{\partial z}\frac{\partial\delta w}{\partial z}\\&+C_{12}(z,T)\left[\frac{\partial u}{\partial z}+\frac{\partial w}{\partial x}\right]\left[\frac{\partial\delta u}{\partial z}+\frac{\partial\delta w}{\partial x}\right]\\&+\rho(z,T)\ddot{u}\delta u+\rho(z,T)\ddot{w}\delta w\Big]dA\\&-\int_A t[B]^T\{\sigma^{th}\}dA\\&-\int_A t\ [b_x\delta u+b_z\delta w]dA-\int_\Gamma P(t)\delta w\ d\Gamma=0\end{aligned} \tag{10}$$

in which b_x and b_z are the body force components in x and z direction; respectively, $\ddot{u}$ and $\ddot{w}$ are the acceleration components, t is the beam thickness. The finite element method is adpted as an efficient numerical tool to solve the considered problem, Chakraborty *et al.* (2003). The Twelve-node 2D-plane element model, as illustrated in Fig. 2, Pantuso *et al.* (2000).

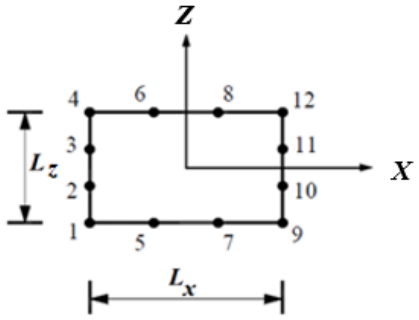

Fig. 2 Twelve-node 2D plane element

where L_x and L_y are element lengths in X and Z directions, respectively. The displacement vector for Twelve-node plane element is expressed as:

$$\{d\} = [\emptyset]\{d_n\} \tag{11a}$$

$$[\emptyset] = [\emptyset_1 \;\; \emptyset_2 \ldots . \emptyset_{12}] \tag{11b}$$

where $\{d_n\}$ indicates the node displacement vector.

$$\{d_n\} = [u_1 \;\; u_2 \;\; . \;\; . \;\; . \;\; u_{12} \;\; w_1 \;\; w_2 \;\; . \;\; . \;\; . \;\; w_{12}]^T \tag{12}$$

where $\{d_n\}$ is the node displacement vector and its components are u_i and w_i are the displacement components for i node. The displacement of any generic element can be represented by its nodal values and corresponding functions as,

$$\begin{aligned} u = (&u_1\emptyset_1 + u_2\emptyset_2 + u_3\emptyset_3 + u_4\emptyset_4 + u_5\emptyset_5 + u_6\emptyset_6 + u_7\emptyset_7 \\ &+ u_8\emptyset_8 + u_9\emptyset_9 + u_{10}\emptyset_{10} \\ &+ u_{11}\emptyset_{11} + u_{12}\emptyset_{12}) \end{aligned} \tag{13a}$$

$$\begin{aligned} w = (&w_1\emptyset_1 + w_2\emptyset_2 + w_3\emptyset_3 + w_4\emptyset_4 + w_5\emptyset_5 + w_6\emptyset_6 \\ &+ w_7\emptyset_7 + w_8\emptyset_8 + w_9\emptyset_9 \\ &+ w_{10}\emptyset_{10} + w_{11}\emptyset_{11} \\ &+ w_{12}\emptyset_{12}) \end{aligned} \tag{13b}$$

where $\emptyset_i$ is the nonlinear interpolation shape functions, which can be represeanted as follows;

$$\begin{aligned}
\emptyset_1 &= \tfrac{1}{32}\left(1-\tfrac{2X}{L_x}\right)\left(1-\tfrac{2Z}{L_z}\right)\left(-10+9\left(\tfrac{4X^2}{L_x{}^2}+\tfrac{4Z^2}{L_z{}^2}\right)\right) & \emptyset_2 &= \tfrac{9}{32}\left(1-\tfrac{2X}{L_x}\right)\left(1-\tfrac{4Z^2}{L_z{}^2}\right)\left(1-\tfrac{6Z}{L_z}\right) \\
\emptyset_3 &= \tfrac{9}{32}\left(1-\tfrac{2X}{L_x}\right)\left(1-\tfrac{4Z^2}{L_z{}^2}\right)\left(1+\tfrac{6Z}{L_z}\right) & \emptyset_4 &= \tfrac{1}{32}\left(1-\tfrac{2X}{L_x}\right)\left(1+\tfrac{2Z}{L_z}\right)\left(-10+9\left(\tfrac{4X^2}{L_x{}^2}+\tfrac{4Z^2}{L_z{}^2}\right)\right) \\
\emptyset_5 &= \tfrac{9}{32}\left(1-\tfrac{2Z}{L_z}\right)\left(1-\tfrac{4X^2}{L_x{}^2}\right)\left(1-\tfrac{6X}{L_x}\right) & \emptyset_6 &= \tfrac{9}{32}\left(1+\tfrac{2Z}{L_z}\right)\left(1-\tfrac{4X^2}{L_x{}^2}\right)\left(1-\tfrac{6X}{L_x}\right) \\
\emptyset_7 &= \tfrac{9}{32}\left(1-\tfrac{2Z}{L_z}\right)\left(1-\tfrac{4X^2}{L_x{}^2}\right)\left(1+\tfrac{6X}{L_x}\right) & \emptyset_8 &= \tfrac{9}{32}\left(1+\tfrac{2Z}{L_z}\right)\left(1-\tfrac{4X^2}{L_x{}^2}\right)\left(1+\tfrac{6X}{L_x}\right) \\
\emptyset_9 &= \tfrac{1}{32}\left(1+\tfrac{2X}{L_x}\right)\left(1-\tfrac{2Z}{L_z}\right)\left(-10+9\left(\tfrac{4X^2}{L_x{}^2}+\tfrac{4Z^2}{L_z{}^2}\right)\right) & \emptyset_{10} &= \tfrac{9}{32}\left(1+\tfrac{2X}{L_x}\right)\left(1-\tfrac{4Z^2}{L_z{}^2}\right)\left(1-\tfrac{6Z}{L_z}\right) \\
\emptyset_{11} &= \tfrac{9}{32}\left(1+\tfrac{2X}{L_x}\right)\left(1-\tfrac{4Z^2}{L_z{}^2}\right)\left(1+\tfrac{6Z}{L_z}\right) & \emptyset_{12} &= \tfrac{1}{32}\left(1+\tfrac{2X}{L_x}\right)\left(1+\tfrac{2Z}{L_z}\right)\left(-10+9\left(\tfrac{4X^2}{L_x{}^2}+\tfrac{4Z^2}{L_z{}^2}\right)\right)
\end{aligned} \tag{14}$$

Substituting Eqs. (4), (11)-(14) into Eq. (10), the dynamic equilibrium equation is rewritten as follows;

$$\begin{aligned} &\int_A \{\delta d_n\}^T\left([B]^T[C][B]\{d_n\} + \rho(Z)[\emptyset]^T[\emptyset]\{\delta\ddot{d}\}\right)dA \\ &-\int_\Gamma \{\delta d_n\}^T[\emptyset]^T P(t)d\Gamma - t\int_A \{\delta d_n\}^T[\emptyset]^T\begin{Bmatrix} b_X \\ b_z \end{Bmatrix}dA = 0 \end{aligned} \tag{15}$$

where

$$[B] = \begin{bmatrix} \frac{\partial}{\partial X} & 0 \\ 0 & \frac{\partial}{\partial Y} \\ \frac{\partial}{\partial Y} & \frac{\partial}{\partial X} \end{bmatrix}[\emptyset],\; [C] = \begin{bmatrix} C_{11}(z,T) & C_{12}(z,T) & 0 \\ C_{12}(z,T) & C_{22}(z,T) & 0 \\ 0 & 0 & C_{33}(z,T) \end{bmatrix} \tag{16}$$

After regulation of Eq. (11a), the dynamic equilibrium equation written as follows:

$$[K]\{d_n\} + [M]\{\ddot{d}_n\} = \{F\} \tag{17}$$

where $[K]$, $[M]$, $\{F\}$ and $\{d_n\}$ are the stiffness matrix, mass matrix, load vector and displacement vector, respectively.

The expansions of finite element matrices are represented as

$$[M] = t\int_A \rho(z)[\emptyset]^T[\emptyset]dA\,,\; [K] = t\int_A [B]^T[C][B]dA \tag{18a}$$

$$\begin{aligned} \{F\} = t\int_A [B]^T[\{\sigma\}^{th}]\,dA + \int_\Gamma \{\delta d_n\}^T[\emptyset]^T P(t)d\Gamma + \\ t\int_A \{\delta d_n\}^T[\emptyset]^T\begin{Bmatrix} b_X \\ b_z \end{Bmatrix}dA \end{aligned} \tag{18b}$$

with $\{\sigma\}^{th}$ is the thermal stress vecor which is given by

$$\{\sigma\}^{th} = \begin{bmatrix} C_{11}(z,T) & C_{12}(z,T) & 0 \\ C_{12}(z,T) & C_{22}(z,T) & 0 \\ 0 & 0 & C_{33}(z,T) \end{bmatrix}\begin{Bmatrix} \alpha(z,T)\Delta T(z) \\ \alpha(z,T)\Delta T(z) \\ 0 \end{Bmatrix} \tag{18c}$$

The dynamic point load $P(t)$ is assumed to be sinusoidal harmonic in time domain as following.

$$\underset{\text{Harmonic}}{(t) = P_0 sin(\Omega t)} \qquad 0 \le t \ll \infty \tag{19}$$

where, P_0 is the amplitude of the dynamic load and Ω is the frequency of the dynamic load. In the solution of Eq. (17), implicit Newmark average acceleration ($\alpha = 0.5$ and $\beta = 0.25$) method is used in the time domain. In this procedure, the dynamic problem is transferred to system of static problem in each step as following

$$[\bar{K}]\{d_n\}_{j+1} = \{\bar{F}(t)\} \tag{20}$$

in which

$$\begin{aligned} [\bar{K}] = [K] + a_0[M] \text{ and } &\{\bar{F}(t)\} \\ &= \{\bar{F}(t)\}_{j+1} \\ &+ [M]\left(a_0\{d_n\}_j + a_1\{\dot{d}_n\}_j + a_2\{\ddot{d}_n\}_j\right) \end{aligned} \tag{21}$$

and constant coefficients can be evaluated by

$$a_0 = \frac{1}{\beta\Delta t^2}\;, \qquad a_1 = \frac{1}{\beta\Delta t}\;, \qquad a_2 = \frac{1-2\beta}{\beta}\;, \tag{22}$$

After evaluating $\{d_n\}_{j+1}$ at a time $t_{j+1} = t_j + \Delta t$, the acceleration and velocity vectors can be evaluated by

$$\{\ddot{d}_n\}_{j+1} = a_0\left(\{d_n\}_{j+1} - \{d_n\}_j\right) - a_1\{\dot{d}_n\}_j - a_2\{\ddot{d}_n\}_j \tag{23a}$$

$$\{\dot{d}_n\}_{j+1} = \{\dot{d}_n\}_j + a_3\{\ddot{d}_n\}_j + a_4\{\ddot{d}_n\}_{j+1} \tag{23b}$$

where $a_3 = (1-\alpha)\Delta t$, and $a_4 = \alpha\Delta t$.

4. Numerical results

In this section, effects of temperature, graduation parameter, geometrical and stacking sequence of layers on the time response of multilayered FGM deep beams. The beams considered in numerical examples are made of Zirconia and aluminium oxide. The FGM layer's bottom

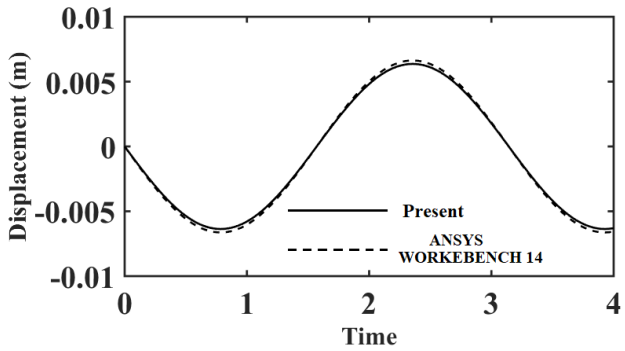

Fig. 3 Comparison study: Time responses of the fully Aluminium Oxide beam for L/h=4, P_0=1000 kN, Ω=2 rad/s, ΔT=100 K

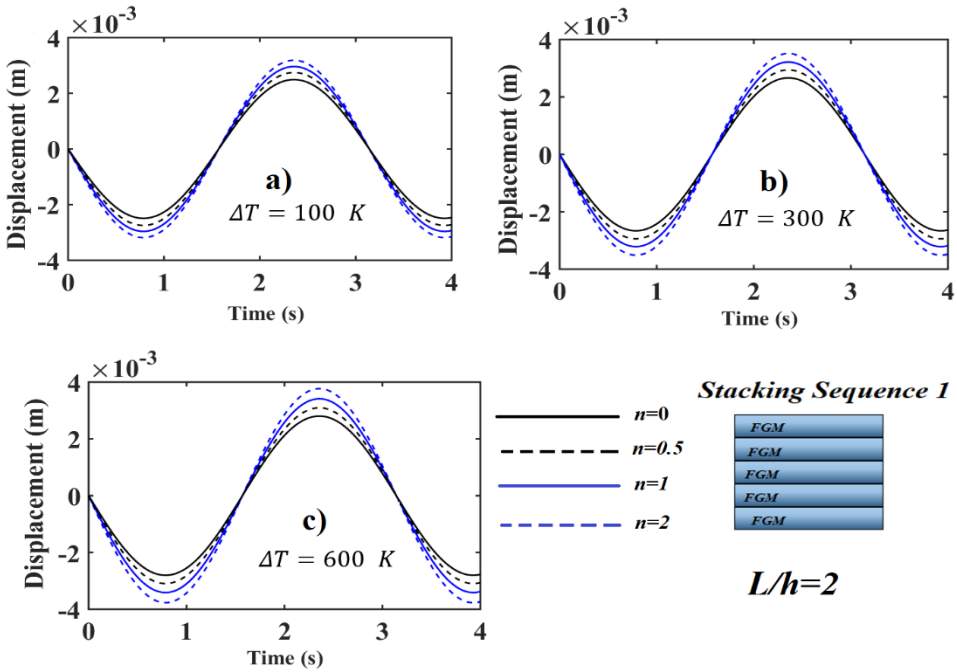

Fig. 4 Time responses of thick FG multi-layered deep beam in *stacking sequence 1* with different *n* parameters for L/h=2 for (a) ΔT=100 K, (b) ΔT=300 K and (c) ΔT=600 K

surface is Zirconia; the top surface material of the FG layer is aluminium. The FGM deep beam dimensions are considered as follows: t = 0.1 m, h = 0.1 m, nd the length of beam varied according to aspect ratios and the length of beam varied according to aspect ratios L/h=2 and 4 in the numerical process. The temperature unit is used as Kelvin (K). The height of each layer is equal to the other. In numerical examples, the initial temperature is assumed to be T_0=300 K. The five-point Gauss rule is used for the calculation of the integration. In the analysis, four different stacking sequences of layers are considered. The stacking sequences of layers used are ***stacking sequence* 1:** five FGM layers, ***stacking sequence* 2:** FGM-AL–AL -FGM-FGM, ***stacking sequence* 3:** AL –AL- FGM-Zirconia-Zirconia layers and ***stacking sequence* 4:** FGM –AL - FGM- Zirconia - FGM.

4.1 Verification of the proposed methodology

In order to check and verify the validity of the developed methodology, a comparison study is performed. In the comparison study, the maximum vertical displacements of a fully Aluminum Oxide beam are obtained and compared with ANSYS Workbench 14 program, Thompson and Thompson (2017) for L/h=4, P_0=1000 *KN* ΔT=100 *K*, Ω=2 *rad/s* in Fig. 3. It is seen from Fig. 3, that the results of this study are approximately identical with results of ANSYS Workbench 14 program .

4.2 Parametric studies

Through this section, time responses of multilayered FG deep beam under sinusoidal harmonic load and the uniform temperature rising are investigated for frequency Ω =2 *rad/s*, the amplitude of the dynamic load $P_0 = 1000$ *KN* with 4 stacking sequences and different distribution parameters (n=0, 0.5, 1, and 2) at specific temperature value.

In order to investigate the effect of temperature, stacking sequences and graduation on the dynamic response of

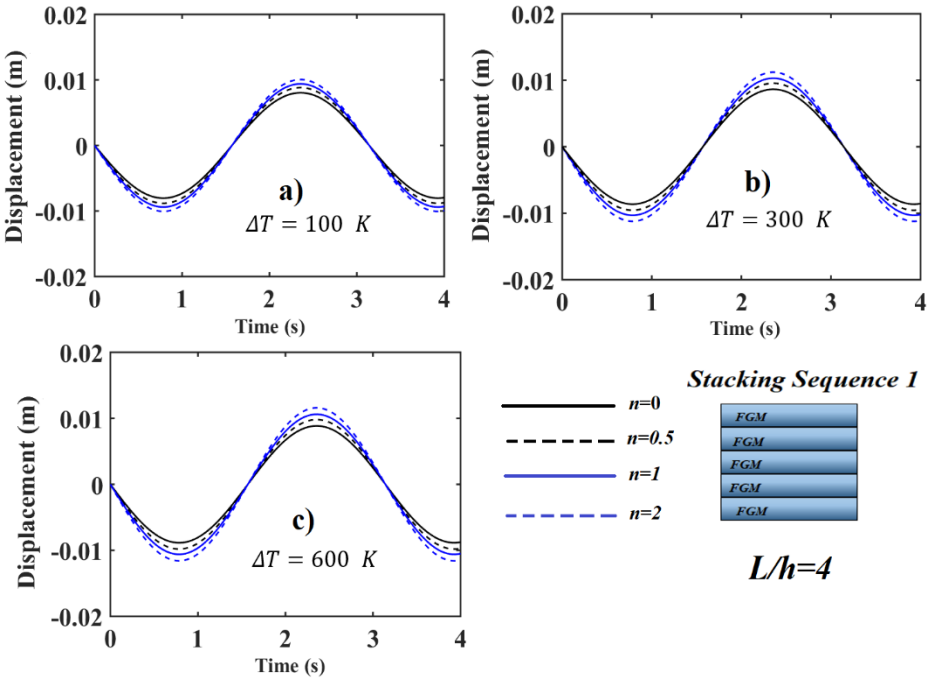

Fig. 5 Time responses of thick FG multi-layered deep beam in *stacking sequence 1* with different *n* parameters for L/h=4 for (a) ΔT=100 K, (b) ΔT=300 K and (c) ΔT=600 K

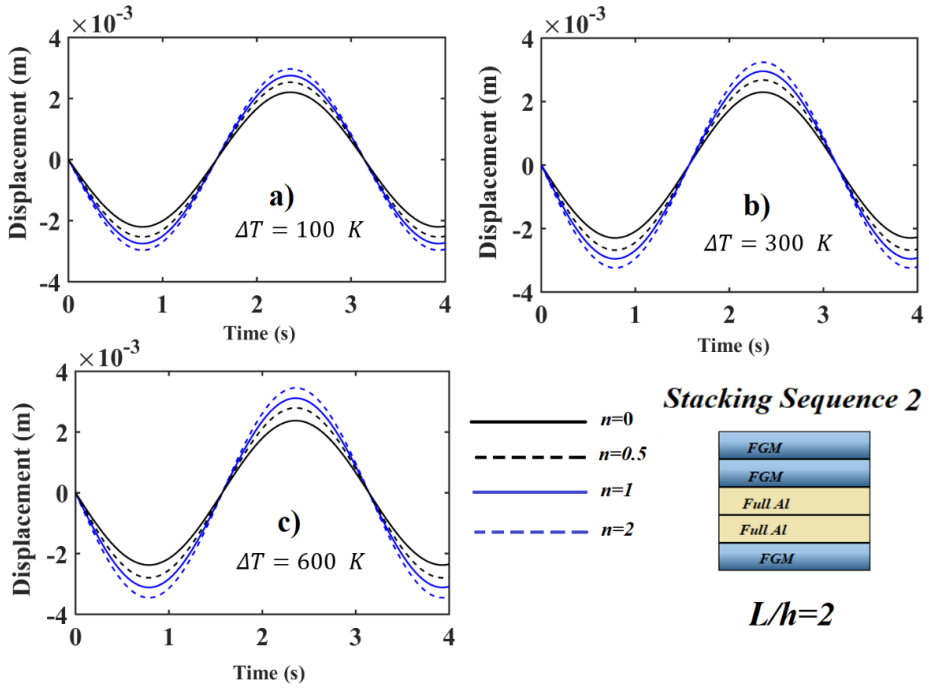

Fig. 6 Time responses of thick FG multi-layered deep beam in *stacking sequence 2* with different *n* parameters for L/h=2 for (a) ΔT=100 K, (b) ΔT=300 K and (c) ΔT=600 K

multilayer FGM deep beam, the dynamical midpoint deflections are presented in Figs. 4-11 for at L/h=2 and L/h=4 in the time history. The results of Stacking sequence 1, Stacking sequence 2, Stacking sequence 3 and Stacking sequence 4 are presented in Figs. 4 and 5, 6 and 7, 8 and 9 and 10-11, respectively. The midpoint deflections are selected to present the dynamic behaviors, because it has the maximum deflections relative to the other points in the domain. As shown in Figs. 4 and 5 for stacking sequence 1, by increasing the gradation index, the deflection is increased due to the softening of the material. However, the time period or frequency is remaining constant because the response of the structure is a steady-state response, and no initial conditions are considered. By increasing the temperature of the environment, the amplitude of response of the beam is increased relatively. That due to the reduction

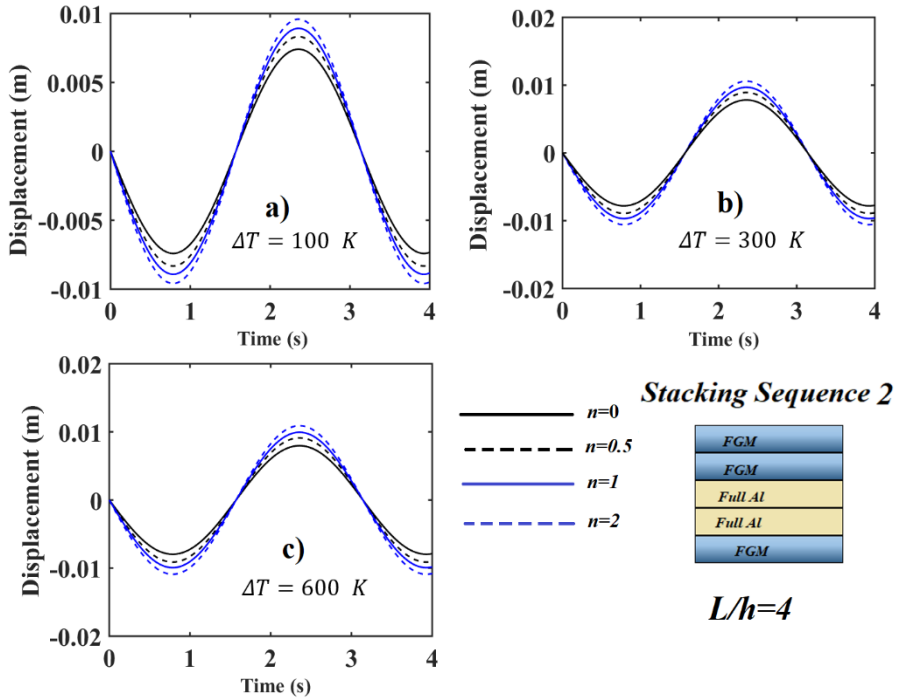

Fig. 7 Time responses of thick FG multi-layered deep beam in *stacking sequence 2* with different *n* parameters for L/h=4 for (a) ΔT=100 K, (b) ΔT=300 K and (c) ΔT=600 K

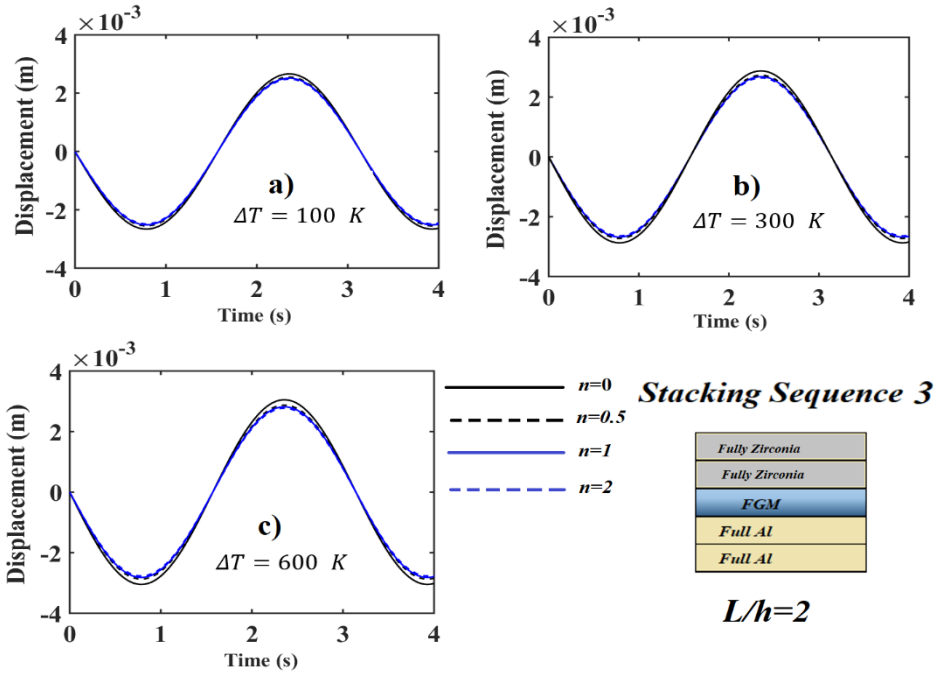

Fig. 8 Time responses of thick FG multi-layered deep beam in *stacking sequence 3* with different *n* parameters for L/h=2 for (a) ΔT=100 K, (b) ΔT=300 K and (c) ΔT=600 K

of elasticity of the graded material since its properties are temperature-dependent. It is also noted that, by increasing the temperature, the effect of gradation on the deflection is increased significantly.

By comparing Figs. 4 and 5 and Figs. 6 and 7, it is noted that same observations predicated in stacking sequence 1 are noticed for stacking sequence 2 as shown in Figs. 5. However, in the case of stacking sequence 3 as presented in Figs. 8 and 9, influences of gradation index and temperature become negligible, that because two layers are purely ceramics and its mechanical properties are not affected by temperature change. In addition, the structure has 4 isotropic layers and only one FG layer. Tthus the gradation index becomes insignificant on the dynamic response of the structure. For stacking sequences 4 shown in Figs 10 and 11, three layers from five are composed of FGMs. Thus, it

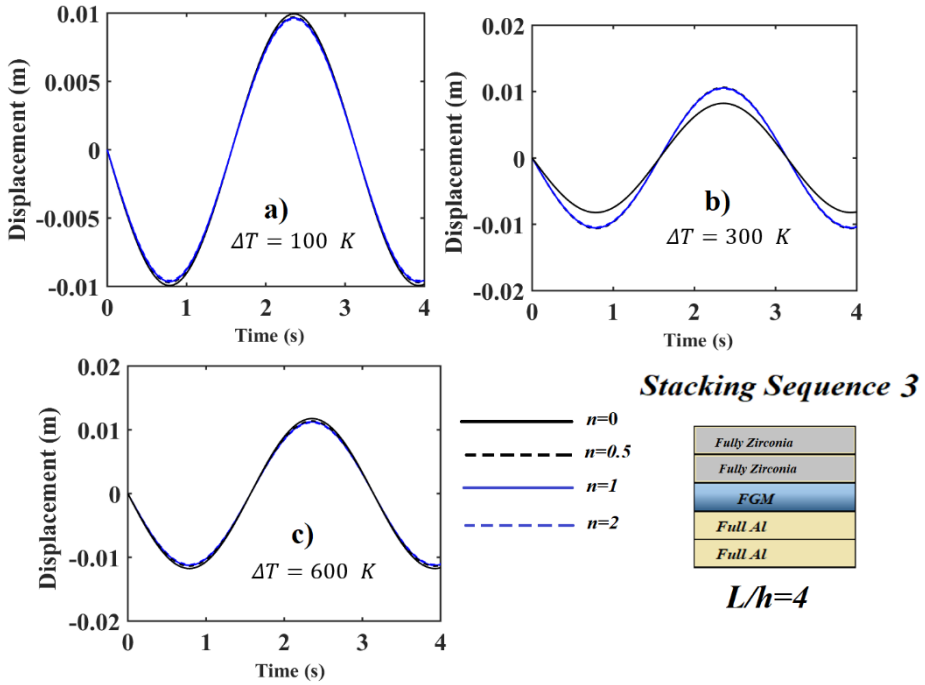

Fig. 9 Time responses of thick FG multi-layered deep beam in *stacking sequence 3* with different *n* parameters for L/h=4 for (a) ΔT=100 K, (b) ΔT=300 K and (c) ΔT=600 K

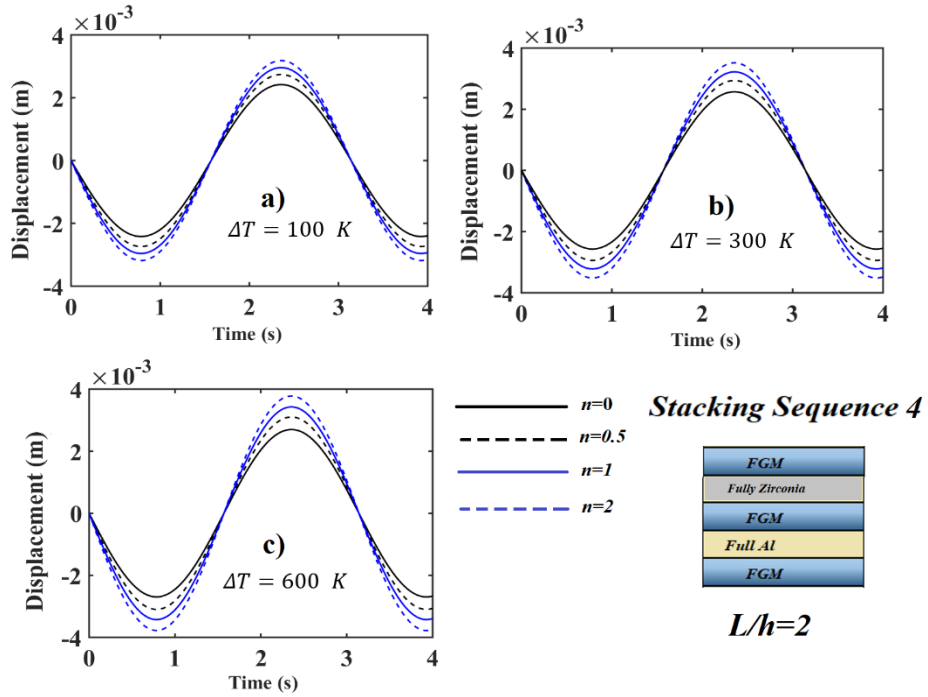

Fig. 10 Time responses of thick FG multi-layered deep beam in *stacking sequence 4* with different *n* parameters for L/h=2 for (a) ΔT=100 K, (b) ΔT=300 K and (c) ΔT=600 K

Is found that the dynamic behavior is dependent on gradation index and temperature as noted for stacking sequences 1 and 2 presented in Figs. 4 and 5 and 6 and 7, respectively.

It is seen from all graphs; the increasing temperature yields to change the dynamic responses significantly. Increasing slenderness ratio tends to increase the response amplitude and may generate a steady-state oscillation response. The effects of the temperature on the dynamic responses vary for different stacking sequences. This situation is observed in the results of stacking sequence 2 and stacking sequence 4. In stacking sequences 2 and 4, the temperature distribution along height direction more vary because of different layer properties. So, the thermal

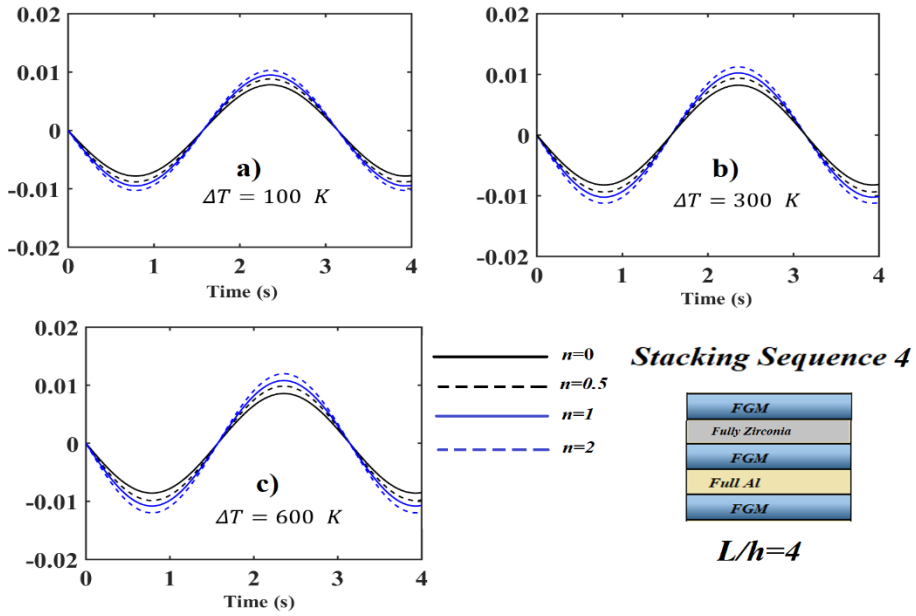

Fig. 11 Time responses of thick FG multi-layered deep beam in *stacking sequence 4* with different *n* parameters for L/h=4 for (a) ΔT=100 K, (b) ΔT=300 K and (c) ΔT=600 K

expansion coefficients change at the layer surfaces discontinuously. As a result of this situation, the bending curvature due to thermal effects more occurs in the stacking sequences 2 and 4.

5. Conclusions

In the framework of two-dimensional thermoelasticity, a dynamic finite element model is developed to study and analyze the thermodynamic response of a multilayered functionally graded deep beam with material temperature dependent under thermomechanical loading. The differential equation of motion and the associated boundary conditions are presented. The dynamic finite element equations are developed. Newmark's implicit technique is adopted to investigate the dynamic time response. The developed procedure is verified through a comparision study with ANSYS benchmark problem and an excellent agreement is observed. Parametric studies are conducted to investigate the effect of temperature, material distribution, and stacking sequence on FG multilayered deep beams' thermodynamic response. The following concluding remarks are revealed:

• The effects of the temperature on the dynamic response vary for different stacking sequences.

• The temperature rising and graduation parameter significantly affects the dynamic deflections, especially for stacking sequences 2 and 4. However, in stacking sequence 3, the graduation parameter has an insignificant effect on vibration amplitude.

• Increasing both slenderness ratio and temperature tends to increase the dynamic response amplitude.

• The dynamic response of deep multilayered beams is siginficantly affected by higher values of temperature rise.

References

Abdelrahman, A.A., Abd-El-Mottaleb, H.E. and Eltaher, M.A. (2020), "On bending analysis of perforated microbeams including the microstructure effects", *Struct. Eng. Mech.*, **76**(6), 765-779. http://doi.org/10.12989/sem.2020.76.6.765.

Abdalrahmaan, A.A., Eltaher, M.A., Kabeel, A.M., Abdraboh, A.M. and Hendi, A.A. (2019), "Free and forced analysis of perforated beams", *Steel Compos. Struct.*, **31**(5), 489-502. https://doi.org/10.12989/scs.2019.31.5.489.

Abdelrahman, A.A. and El-Shafei, A.G. (2020), "Modeling and analysis of the transient response of viscoelastic solids", *Waves Random Complex Media*, 1-31. https://doi.org/10.1080/17455030.2020.1714790.

Abdelrahman, A.A., Mohamed, N.A. and Eltaher, M.A. (2020), "Static bending of perforated nanobeams including surface energy and microstructure effects", *Eng. Comput.*, 1-21. https://doi.org/10.1007/s00366-020-01149-x.

Abdulrazzaq, M.A., Fenjan, R.M., Ahmed, R.A. and Faleh, N.M. (2020), "Thermal buckling of nonlocal clamped exponentially graded plate according to a secant function based refined theory", *Steel Compos. Struct.*, **35**(1), 147-157. https://doi.org/10.12989/scs.2020.35.1.147.

Abo-bakr, R.M., Abo-bakr, H.M., Mohamed, S.A. and Eltaher, M. A. (2020), "Optimal weight for buckling of FG beam under variable axial load using Pareto optimality", *Compos. Struct.*, 113193. https://doi.org/10.1016/j.compstruct.2020.113193.

Abo-bakr, H.M., Abo-bakr, R.M., Mohamed, S.A. and Eltaher, M.A. (2021a), "Multi-objective shape optimization for axially functionally graded microbeams", *Compos. Struct.*, **258**, 113370. https://doi.org/10.1016/j.compstruct.2020.113370.

Abo-Bakr, H.M., Abo-Bakr, R.M., Mohamed, S.A. and Eltaher, M.A. (2020b), "Weight optimization of axially functionally graded microbeams under buckling and vibration behaviors", *Mech. Based Des. Struc.*, 1-22. https://doi.org/10.1080/15397734.2020.1838298 .

Ahmadi, H. and Foroutan, K. (2019), "Effect of the multi vibration absorbers on the nonlinear FG beam under periodic load with various boundary conditions", *J. Solid Mech.*, **11**(3), 523-534.

https://doi.org/10.22034/JSM.2019.666688.
Akbaş, Ş.D. (2016), "Forced vibration analysis of viscoelastic nanobeams embedded in an elastic medium", *Smart Struct. Syst.*, **18**(6), 1125-1143. https://doi.org/10.12989/sss.2016.18.6.1125.
Akbaş, Ş.D. (2017a), "Forced vibration analysis of functionally graded nanobeams", *Int. J. Appl. Mech.*, **9**(7), 1750100. https://doi.org/10.1142/S1758825117501009.
Akbaş, Ş.D. (2017b), "Thermal effects on the vibration of functionally graded deep beams with porosity", *Int. J. Appl. Mech.*, **9**(5), 1750076. https://doi.org/10.1142/S1758825117500764.
Akbaş, Ş.D. (2018a), "Forced vibration analysis of cracked nanobeams", *J. Brazil. Soc. Mech. Sci. Eng.*, **40**(8), 392. https://doi.org/10.1007/s40430-018-1315-1.
Akbaş, Ş.D. (2018b), "Forced vibration analysis of cracked functionally graded microbeams", *Adv. Nano Res.*, **6**(1), 39-55. https://doi.org/10.12989/anr.2018.6.1.039.
Akbas, S.D. (2018c), "Investigation on free and forced vibration of a bi-material composite beam", *J. Polytechnic-Politeknik Dergisi*, **21**(1), 65-73. https://doi.org/10.21923/jesd.553328.
Akbaş, Ş.D. (2019a), "Hygro-thermal nonlinear analysis of a functionally graded beam", *J. Appl. Comput. Mech.*, **5**(2), 477-485. https://dx.doi.org/10.22055/jacm.2018.26819.1360.
Akbas, S.D. (2019b), "Forced vibration analysis of functionally graded sandwich deep beams", *Coupled Syst. Mech.*, **8**(3), 259-271. https://doi.org/10.12989/csm.2019.8.3.259.
Akbaş, S.D., Fageehi, Y.A., Assie, E.A. and Eltaher, M.A. (2020a), "Dynamic analysis of visco-elastic functionally graded porous thick beams under pulse load", *Eng. Comput.*, 1-18. https://doi.org/ 10.1007/s00366-020-01070-3.
Akbaş, Ş.D., Bashiri, H.A., Assie, A.E. and Eltaher, M.A. (2020b), "Dynamic analysis of thick beams with functionally graded porous layers and viscoelastic support", *J. Vib. Control*, 1-12. https://doi.org/10.1177/1077546320947302.
Albino, J.C.R., Almeida, C.A., Menezes, I.F.M. and Paulino, G.H. (2018), "Co-rotational 3D beam element for nonlinear dynamic analysis of risers manufactured with functionally graded materials (FGMs)", *Eng. Struct.*, **173**, 283-299. https://doi.org/10.1016/j.engstruct.2018.05.092.
Almitani, K.H., Abdalrahmaan, A.A., Eltaher, M.A. (2019), "On forced and free vibrations of cutout squared beams", *Steel Compos. Struct.*, **32**(5), 643-655. https://doi.org/10.12989/scs.2019.32.5.643.
Almitani, K.H., Abdalrahmaan, A.A. and Eltaher, M.A. (2020), "Stability of perforated nanobeams incorporating surface energy effects", *Steel Compos. Struct.*, **35**(4), 643-655. https://doi.org/10.12989/scs.2020.35.4.555.
Alnujaie, A., Akbas, Ş.D., Eltaher, M.A. and Assie, A. (2021), "Forced vibration of a functionally graded porous beam resting on viscoelastic foundation", *Geomech. Eng.*, **24**(1), 91-103. https://doi.org/10.12989/gae.2021.24.1.091.
Alshorbagy, A.E., Eltaher, M.A. and Mahmoud, F.F. (2011), "Free vibration characteristics of a functionally graded beam by finite element method", *Appl. Math. Model.*, **35**(1), 412-425. https://doi.org/10.1016/j.apm.2010.07.006.
Arioui, O., Belakhdar, K., Kaci, A. and Tounsi, A. (2018), "Thermal buckling of FGM beams having parabolic thickness variation and temperature dependent materials", *Steel Compos. Struct.*, **27**(6), 777-788. https://doi.org/10.12989/scs.2018.27.6.777.
Assie, A.E., Eltaher, M.A. and Mahmoud, F.F. (2011), "Behavior of a viscoelastic composite plates under transient load", *J. Mech. Sci. Technol.*, **25**(5), 1129. https://doi.org/10.1007/s12206-011-0302-6.
Assie, A., Akbaş, Ş.D., Bashiri, A.H., Abdelrahman, A.A. and Eltaher, M.A. (2021), "Vibration response of perforated thick beam under moving load", *Eur. Phys. J. Plus*, **136**(3), 1-15. https://doi.org/10.1140/epjp/s13360-021-01224-2.
Attia, M.A. and Abdelrahman, A.A. (2018), "On vibrations of functionally graded viscoelastic nanobeams with surface effects", *Int. J. Eng. Sci.*, **127**, 1-32. https://doi.org/10.1016/j.ijengsci.2018.02.005.
Attia, M.A., Eltaher, M.A., Soliman, A., Abdelrahman, A.A. and Alshorbagy, A.E. (2018), "Thermoelastic crack analysis in functionally graded pipelines conveying natural gas by an FEM", *Int. J. Appl. Mech.*, **10**(4), 1850036. https://doi.org/10.1142/S1758825118500369.
Barka, M., Benrahou, K.H., Bakora, A. and Tounsi, A. (2016), "Thermal post-buckling behavior of imperfect temperature-dependent sandwich FGM plates resting on Pasternak elastic foundation", *Steel Compos. Struct.*, **22**(1), 91-112. https://doi.org/10.12989/scs.2016.22.1.091.
Berghouti, H., Adda Bedia, E.A., Benkhedda, A. and Tounsi, A. (2019), "Vibration analysis of nonlocal porous nanobeams made of functionally graded material", *Adv. Nano Res.*, **7**(5), 351-364. https://doi.org/10.12989/anr.2019.7.5.351.
Chakraborty, A., Gopalakrishnan, S. and Reddy, J.N. (2003), "A new beam finite element for the analysis of functionally graded materials", *Int. J. Mech. Sci.*, **45**(3), 519-539. https://doi.org/10.1016/S0020-7403(03)00058-4.
Chen, Y., Jin, G., Zhang, C., Ye, T. and Xue, Y. (2018), "Thermal vibration of FGM beams with general boundary conditions using a higher-order shear deformation theory", *Compos. Part B Eng.*, **153**, 376-386.| https://doi.org/10.1016/j.compositesb.2018.08.111.
Dinh Duc, N., Quang, V.D., Nguyen, P.D. and Chien, T.M. (2018), "Nonlinear dynamic response of functionally graded porous plates on elastic foundation subjected to thermal and mechanical loads", *J. Appl. Comput. Mech.*, **4**(4), 245-259. https://doi.org/10.22055/JACM.2018.23219.1151.
Doroushi, A., Eslami, M.R. and Komeili, A. (2011), "Vibration analysis and transient response of an FGPM beam under thermo-electro-mechanical loads using higher-order shear deformation theory", *J. Intell. Mat. Syst.*, **22**(3), 231-243. https://doi.org/10.1177/1045389X11398162.
Ebrahimi, F., Fardshad, R.E. and Mahesh, V. (2019), "Frequency response analysis of curved embedded magneto-electro-viscoelastic functionally graded nanobeams", *Adv. Nano Res.*, **7**(6), 391-403. https://doi.org/10.12989/anr.2019.7.6.391.
Ebrahimi, F., Jafari, A. and Selvamani, R. (2020), "Thermal buckling analysis of magneto-electro-elastic porous FG beam in thermal environment", *Adv. Nano Res.*, **8**(1), 83-94. https://doi.org/10.12989/anr.2020.8.1.083
Eltaher, M.A., Alshorbagy, A.E. and Mahmoud, F.F. (2013a), "Determination of neutral axis position and its effect on natural frequencies of functionally graded macro/nanobeams", *Compos. Struct.*, **99**, 193-201. https://doi.org/10.1016/j.compstruct.2012.11.039.
Eltaher, M.A., Mahmoud, F.F., Assie, A.E. and Meletis, E.I. (2013b), "Coupling effects of nonlocal and surface energy on vibration analysis of nanobeams", *Appl. Math. Comput.*, **224**, 760-774. https://doi.org/10.1016/j.amc.2013.09.002.
Eltaher, M.A., Attia, M.A., Soliman, A.E. and Alshorbagy, A.E. (2018), "Analysis of crack occurs under unsteady pressure and temperature in a natural gas facility by applying FGM", *Struct. Eng. Mech.*, **66**(1), 97-111. https://doi.org/10.12989/sem.2018.66.1.097.
Eltaher, M.A. and Mohamed, S.A. (2020), "Buckling and stability analysis of sandwich beams subjected to varying axial loads", *Steel Compos. Struct.*, **34**(2), 241-260. http://doi.org/10.12989/scs.2020.34.2.241.
Eltaher, M.A. and Akbas, Ş.D. (2020), "Transient response of 2D functionally graded beam structure", *Struct. Eng. Mech.*, **75**(3),

357-367. https://doi.org/10.12989/sem.2020.75.3.357.
Eltaher, M.A., Mohamed, S.A. and Melaibari, A. (2020a), "Static stability of a unified composite beams under varying axial loads", *Thin-Walled Struct*., **147**, 106488. https://doi.org/10.1016/j.tws.2019.106488.
Emam, S. and Eltaher, M.A. (2016), "Buckling and postbuckling of composite beams in hygrothermal environments", *Compos. Struct*., **152**, 665-675. https://doi.org/10.1016/j.compstruct.2016.05.029.
Emam, S., Eltaher, M., Khater, M. and Abdalla, W. (2018), "Postbuckling and free vibration of multilayer imperfect nanobeams under a pre-stress load", *Appl. Sci*., **8**(11), 2238. https://doi.org/10.3390/app8112238.
Esen, I., Özarpa, C. and Eltaher, M.A. (2021), "Free vibration of a cracked FG microbeam embedded in an elastic matrix and exposed to magnetic field in a thermal environment", *Compos. Struct*., **261**, 113552. https://doi.org/10.1016/j.compstruct.2021.113552.
Gan, B.S., Trinh, T.H., Le, T.H. and Nguyen, D.K. (2015), "Dynamic response of non-uniform Timoshenko beams made of axially FGM subjected to multiple moving point loads", *Struct. Eng. Mech*., **53**(5), 981-995. https://doi.org/10.12989/sem.2015.53.5.981.
Ganczarski, A. and Szubartowski, D. (2019), "Conditions of stress-free deformation of anisotropic FGM interface under constant temperature", *J. Therm. Stresses*, **42**(1), 152-162. https://doi.org/10.1080/01495739.2018.1536868.
Ghadiri, M., Shafiei, N. and Babaei, R. (2017), "Vibration of a rotary FG plate with consideration of thermal and Coriolis effects", *Steel Compos. Struct*., **25**(2), 197-207. https://doi.org/10.12989/scs.2017.25.2.197.
Gupta, A. and Talha, M. (2015), "Recent development in modeling and analysis of functionally graded materials and structures", *Progress Aerosp. Sci*., **79**, 1-14. https://doi.org/10.1016/j.paerosci.2015.07.001.
Hamed, M.A., Sadoun, A.M. and Eltaher, M.A. (2019), "Effects of porosity models on static behavior of size dependent functionally graded beam", *Struct. Eng. Mech*., **71**(1), 89-98. https://doi.org/10.12989/sem.2019.71.1.089.
Hamed, M.A., Abo-bakr, R.M., Mohamed, S.A. and Eltaher, M.A. (2020a), "Influence of axial load function and optimization on static stability of sandwich functionally graded beams with porous core", *Eng. Comput*., **36**(4), 1929-1946. https://doi.org/10.1007/s00366-020-01023-w.
Hamed M.A., Mohamed, S.A., Eltaher, M.A. (2020b), "Buckling analysis of sandwich beam rested on elastic foundation and subjected to varying axial in-plane loads", *Steel Compos. Struct*., **34**(2), 75-89. https://doi.org/10.12989/scs.2020.34.1.075.
Hamidi, B.A., Hosseini, S.A., Hayati, H. and Hassannejad, R. (2020), "Forced axial vibration of micro and nanobeam under axial harmonic moving and constant distributed forces via nonlocal strain gradient theory", *Mech. Based Des. Struc*., 1-15. https://doi.org/10.1080/15397734.2020.1744003.
Hemmatnezhad, M., Ansari, R. and Rahimi, G.H. (2013), "Large-amplitude free vibrations of functionally graded beams by means of a finite element formulation", *Appl. Math. Modell*., **37**(18-19), 8495-8504. https://doi.org/10.1016/j.apm.2013.03.055.
Hosseini, S.A.H. and Rahmani, O. (2016), "Free vibration of shallow and deep curved FG nanobeam via nonlocal Timoshenko curved beam model", *Appl. Phys. A*, **122**(3), 169. https://doi.org/10.1007/s00339-016-9696-4.
Karami, B., Shahsavari, D., Nazemosadat, S.M.R., Li, L. and Ebrahimi, A. (2018), "Thermal buckling of smart porous functionally graded nanobeam rested on Kerr foundation" *Steel Compos. Struct*., **29**(3), 349-362. https://doi.org/10.12989/scs.2018.29.3.349.
Lee, Y.D. and Erdogan, F. (1994), "Residual/thermal stresses in FGM and laminated thermal barrier coatings", *Int. J. Fract*., **69**(2), 145-165. https://doi.org/10.1007/BF00035027.
Malekzadeh, P. and Monajjemzadeh, S.M. (2013), "Dynamic response of functionally graded plates in thermal environment under moving load", *Compos. Part B Eng*., **45**(1), 1521-1533. https://doi.org/10.1016/j.compositesb.2012.09.022.
Mirjavadi, S.S., Afshari, B.M., Shafiei, N., Hamouda, A.M.S. and Kazemi, M. (2017), "Thermal vibration of two-dimensional functionally graded (2D-FG) porous Timoshenko nanobeams", *Steel Compos. Struct*., **25**(4), 415-426. https://doi.org/10.12989/scs.2017.25.4.415.
Mohamed, N., Eltaher, M.A., Mohamed, S. and Seddek, L.F. (2019), "Energy equivalent model in analysis of postbuckling of imperfect carbon nanotubes resting on nonlinear elastic foundation", *Struct. Eng. Mech*., **70**(6), 737-750. https://doi.org/10.12989/sem.2019.70.6.737.
Rahman, M., Hasan, A.S. and Yeasmin, I.A. (2019), "Modified multi-level residue harmonic balance method for solving nonlinear vibration problem of beam resting on nonlinear elastic foundation", *J. Appl. Comput. Mech*., **5**(4), 627-638. https://doi.org/10.22055/JACM.2018.26729.1352.
Pantuso, D., Bathe, K.J. and Bouzinov, P.A. (2000), "A finite element procedure for the analysis of thermo-mechanical solids in contact", *Comput. Struct*., **75**(6), 551-573. https://doi.org/10.1016/S0045-7949(99)00212-6.
Rajasekaran, S. and Khaniki, H.B. (2019), "Size-dependent forced vibration of non-uniform bi-directional functionally graded beams embedded in variable elastic environment carrying a moving harmonic mass", *Appl. Math. Model*., **72**, 129-154. https://doi.org/10.1016/j.apm.2019.03.021.
Reddy, J.N. and Chin, C.D. (1998), "Thermomechanical analysis of functionally graded cylinders and plates", *J. Therm. Stresses*, **21**(6), 593-626. https://doi.org/10.1080/01495739808956165.
Salah, F., Boucham, B., Bourada, F., Benzair, A., Bousahla, A.A. and Tounsi, A. (2019), "Investigation of thermal buckling properties of ceramic-metal FGM sandwich plates using 2D integral plate model", *Steel Compos. Struct*., **33**(6), 805-822. https://doi.org/10.12989/scs.2019.33.6.805.
Sedighi, H. M. (2014), "Size-dependent dynamic pull-in instability of vibrating electrically actuated microbeams based on the strain gradient elasticity theory", *Acta Astronautica*, **95**, 111-123. https://doi.org/10.1016/j.actaastro.2013.10.020.
Sedighi, H.M., Shirazi, K.H. and Noghrehabadi, A. (2012), "Application of recent powerful analytical approaches on the non-linear vibration of cantilever beams", *Int. J. Nonlin Sci. Numer. Simul*., **13**(7-8), 487-494. https://doi.org/10.1515/ijnsns-2012-0030.
Sedighi, H. M., Koochi, A., Daneshmand, F. and Abadyan, M. (2015), "Non-linear dynamic instability of a double-sided nano-bridge considering centrifugal force and rarefied gas flow", *Int. J. Non-Linear Mech*., **77**, 96-106. https://doi.org/10.1016/j.ijnonlinmec.2015.08.002.
Sedighi, H.M. and Bozorgmehri, A. (2016), "Dynamic instability analysis of doubly clamped cylindrical nanowires in the presence of Casimir attraction and surface effects using modified couple stress theory", *Acta Mechanica*, **227**(6), 1575-1591. https://doi.org/10.1007/s00707-016-1562-0.
She, G.L. (2020), "Wave propagation of FG polymer composite nanoplates reinforced with GNPs", *Steel Compos. Struct*, **37**(1), 27-35. https://doi.org/10.12989/scs.2020.37.1.027.
She, G.L., Liu, H.B. and Karami, B. (2021), "Resonance analysis of composite curved microbeams reinforced with graphene nanoplatelets", *Thin-Walled Struct*., **160**, 107407. https://doi.org/10.1016/j.tws.2020.107407.
Şimşek, M. and Kocatürk, T. (2009), "Free and forced vibration of

a functionally graded beam subjected to a concentrated moving harmonic load", *Compos*. *Struct*., **90**(4), 465-473. https://doi.org/10.1016/j.compstruct.2009.04.024.

Şimşek, M. (2010). "Vibration analysis of a functionally graded beam under a moving mass by using different beam theories", *Compos*. *Struct*., **92**(4), 904-917. https://doi.org/10.1016/j.compstruct.2009.09.030.

Soliman, A.E., Eltaher, M.A., Attia, M.A. and Alshorbagy, A.E. (2018), "Nonlinear transient analysis of FG pipe subjected to internal pressure and unsteady temperature in a natural gas facility", *Struct*. *Eng*. *Mech*., **66**(1), 85-96. https://doi.org/10.12989/sem.2018.66.1.085.

Thompson, M.K. and Thompson, J.M. (2017), *ANSYS Mechanical APDL for Finite Element Analysis*, Butterworth-Heinemann.

Touloukian, Y.S. (1966), "Thermophysical properties of high temperature solid materials. Volume 5. nonoxides and their solutions and mixtures, including miscellaneous ceramic materials", AD0649953, Thermophysical and Electronic Properties In-formation Analysis Center Lafayette, U.S.A.

Tsiptsis, I.N. and Sapountzaki, O.E. (2019), "Beam & shell models for composite straight or curved bridge decks with intermediate diaphragms & assessment of design specifications", *J*. *Appl*. *Comput*. *Mech*., **5**(5), 998-1022. https://doi.org/10.22055/JACM.2019.28743.1502.

Ueda, S. and Mizusawa, S. (2020), "An axisymmetric crack in a functionally graded thermal barrier coating bonded to a homogeneous elastic substrate under transient thermal loading", *J*. *Therm*. *Stresses*, **43**(8), 940-961. https://doi.org/10.1080/01495739.2020.1755614.

Wang, H. and Qin, Q.H. (2008), "Meshless approach for thermo-mechanical analysis of functionally graded materials", *Eng*. *Anal*. *Boundary Elements*, **32**(9), 704-712. https://doi.org/10.1016/j.enganabound.2007.11.001.

Wang, Y. and Wu, D. (2016), "Thermal effect on the dynamic response of axially functionally graded beam subjected to a moving harmonic load", *Acta Astronautica*, **127**, 171-181. https://doi.org/10.1016/j.actaastro.2016.05.030.

Xiang, H.J. and Yang, J. (2008), "Free and forced vibration of a laminated FGM Timoshenko beam of variable thickness under heat conduction", *Compos*. *Part B Eng*., **39**(2), 292-303. https://doi.org/10.1016/j.compositesb.2007.01.005.

Yang, J., Chen, Y., Xiang, Y. and Jia, X.L. (2008), "Free and forced vibration of cracked inhomogeneous beams under an axial force and a moving load", *J*. *Sound Vib*., **312**(1-2), 166-181. https://doi.org/10.1016/j.jsv.2007.10.034.

Zenkour, A.M. and Abouelregal, A.E. (2014), "The effect of two temperatures on a FG nanobeam induced by a sinusoidal pulse heating", *Struct*. *Eng*. *Mech*., **51**(2), 199-214. https://doi.org/10.12989/sem.2014.51.2.199.